

## Selected-fit versus induced-fit protein binding: Kinetic differences and mutational analysis

Thomas R. Weikl and Carola von Deuster

Max Planck Institute of Colloids and Interfaces, Department of Theory  
and Bio-Systems, Science Park Golm, 14424 Potsdam, Germany

The binding of a ligand molecule to a protein is often accompanied by conformational changes of the protein. A central question is whether the ligand induces the conformational change (induced-fit), or rather selects and stabilizes a complementary conformation from a pre-existing equilibrium of ground and excited states of the protein (selected-fit). We consider here the binding kinetics in a simple four-state model of ligand-protein binding. In this model, the protein has two conformations, which can both bind the ligand. The first conformation is the ground state of the protein when the ligand is off, and the second conformation is the ground state when the ligand is bound. The induced-fit mechanism corresponds to ligand binding in the unbound ground state, and the selected-fit mechanism to ligand binding in the excited state. We find a simple, characteristic difference between the on- and off-rates in the two mechanisms if the conformational relaxation into the ground states is fast. In the case of selected-fit binding, the on-rate depends on the conformational equilibrium constant, while the off-rate is independent. In the case of induced-fit binding, in contrast, the off-rate depends on the conformational equilibrium, while the on-rate is independent. Whether a protein binds a ligand via selected-fit or induced-fit thus may be revealed by mutations far from the protein's binding pocket, or other "perturbations" that only affect the conformational equilibrium. In the case of selected-fit, such mutations will only change the on-rate, and in the case of induced-fit, only the off-rate.

### INTRODUCTION

The function of a protein often requires dynamic changes between different three-dimensional conformations. Conformational changes that occur when a protein binds a ligand molecule are well documented by experimentally determined structures of proteins in the unbound state and the ligand-bound state [1, 2]. In 1958, Koshland [3] suggested that the binding of the ligand may induce the conformational change of the protein. More recently, Tsai *et al.* [4, 5] suggested an alternative mechanism in which the ligand selects and stabilizes a complementary protein conformation from an equilibrium of low-energy and higher-energy conformations. This selected-fit, or conformational selection mechanism is based on the energy-landscape picture of protein folding [6, 7].

How can we distinguish whether a protein binds its ligand in an induced-fit or selected-fit mechanism? Recent single-molecule fluorescence [8, 9, 10, 11, 12, 13] and NMR relaxation experiments [14, 15, 16, 17, 18] provide dynamic insights into conformational transitions. NMR relaxation experiments of the enzyme DHFR, which binds two ligands, reveal excited-state conformations that resemble ground-state conformations of adjacent ligand-bound or ligand-free states on the catalytic cycle [16]. These experiments provide evidence for a pre-existing equilibrium of conformations that is shifted by the binding or unbinding of a ligand, as suggested in the selected-fit mechanism of protein binding [4, 5]. For the binding of myosin to actin, in contrast, an induced-fit mechanism has been proposed [2] based on cryo-microscopic images of the actin-myosin complex [19].

We consider here the selected-fit and induced-fit binding kinetics in a simple four-state model of protein-ligand binding (see fig. 1). In this model, the protein, or enzyme, has two dominant conformations  $E_1$  and  $E_2$ . The conformation  $E_1$  is the ground-state conformation in the unbound state of

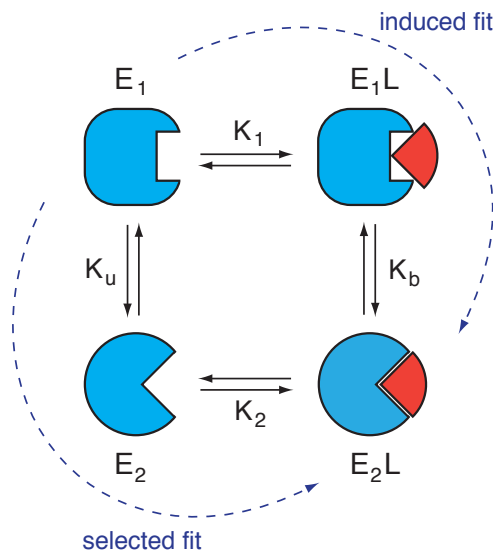


FIG. 1: Simple four-state model of protein-ligand binding. Without the ligand  $L$ , the conformation  $E_1$  of the protein, or enzyme, is the ground-state conformation, and  $E_2$  is the excited-state conformation. When the ligand is bound,  $E_2L$  is the ground state, and  $E_1L$  the excited state. On the selected-fit route, the ligand binds the protein in the excited-state conformation  $E_2$ , and on the induced-fit binding route, in the ground-state conformation  $E_1$ .

the protein, while  $E_2$  is the ground-state conformation in the ligand-bound state. Two routes connect the unbound ground state  $E_1$  and bound ground state  $E_2L$ . On the induced-fit route  $E_1 \rightarrow E_1L \rightarrow E_2L$ , the protein first binds the ligand in conformation  $E_1$ , which causes the transition into conformation  $E_2$ . On the selected-fit route  $E_1 \rightarrow E_2 \rightarrow E_2L$ , the protein binds the ligand in the higher-energy conformation  $E_2$ .

We find a characteristic difference between the selected-fit

and induced-fit binding kinetics. If the conformational relaxation into the ground state is fast, the selected-fit on-rate depends on the equilibrium constant of the conformations  $E_1$  and  $E_2$ , while the selected-fit off-rate is independent of the conformational equilibrium. The induced-fit on-rate, in contrast, is independent of the conformational equilibrium between  $E_1L$  and  $E_2L$ , whereas the induced-fit off-rate depends on this equilibrium. Mutations or other perturbations that shift the conformational equilibrium without affecting the shape or free energies of the binding site thus may help to identify whether a protein binds its ligand in a selected-fit or induced-fit mechanism.

## RESULTS

### Equilibrium behavior

The four states of our model are connected by four transitions with equilibrium constants  $K_1$ ,  $K_2$ ,  $K_u$ , and  $K_b$  (see fig. 1). In the model, the constants  $K_u$  and  $K_b$  for the conformational equilibrium in the unbound and the bound state obey

$$K_u = \frac{[E_2]}{[E_1]} \ll 1, \quad K_b = \frac{[E_2L]}{[E_1L]} \gg 1 \quad (1)$$

since  $E_1$  is the ground-state conformation in the unbound state of the protein, and  $E_2L$  is the ground state when the ligand is bound. We assume here that the excited-state conformations are significantly higher in free energy than the ground states. The binding equilibrium of the two conformations is governed by the constants

$$K_1 = \frac{[E_1L]}{[E_1][L]}, \quad K_2 = \frac{[E_2L]}{[E_2][L]} \quad (2)$$

From the two equalities  $[E_2L] = K_2[E_2][L] = K_2K_u[E_1][L]$  and  $[E_2L] = K_b[E_1L] = K_bK_1[E_1][L]$  that follow directly from these definitions, we obtain the general relation

$$K_uK_2 = K_bK_1 \quad (3)$$

between the four equilibrium constants. Thus, only three of the equilibrium constants are independent.

The selected-fit route  $E_1 \rightarrow E_2 \rightarrow E_2L$  in our model dominates over the induced-fit route  $E_1 \rightarrow E_1L \rightarrow E_2L$  if the concentration  $[E_2]$  of the selected-fit intermediate is larger than the concentration  $[E_1L]$  of the induced-fit intermediate. Since  $[E_2] = K_u[E_1]$  and  $[E_1L] = K_1[E_1][L]$ , the selected-fit mechanism thus is dominant for small ligand concentrations

$$[L] < K_u/K_1 \quad (4)$$

while the induced-fit mechanism is dominant for large ligand concentrations  $[L] > K_u/K_1$ .

### Selected-fit binding kinetics

We first consider the binding kinetics along the selected-fit route of our model (see figs. 1 and 2). The selected-fit binding rate is the dominant relaxation rate of the process

$$E_1 \xrightleftharpoons[s_{12}]{s_{21}} E_2 \xrightarrow{s_b[L]} E_2L \quad (5)$$

from  $E_1$  to  $E_2L$ , with  $E_2L$  as an ‘‘absorbing state’’ without backflow into  $E_2$ . Here,  $s_{21}$  is the transition rate from state  $E_1$  to  $E_2$ ,  $s_{12}$  is the rate for the reverse transition, and  $s_b$  is the binding rate per mole ligand in state  $E_2$ . In the appendix, we calculate the exact relaxation rates for a process of the form (5). Since  $E_2$  is the excited state, we have  $s_{21}/s_{12} = K_u \ll 1$ , and the on-rate of the selected-fit process (5) is approximately given by

$$s_{\text{on}}[L] \approx \frac{s_{21}s_b[L]}{s_{12} + s_b[L]} \quad (6)$$

(see eq. (25) in the Appendix). For small ligand concentrations  $[L]$ , or fast conformational relaxation  $s_{12}$  into the ground-state conformation  $E_1$ , we have  $s_b[L] \ll s_{12}$ , and the selected-fit on-rate per mole ligand is

$$s_{\text{on}} \approx \frac{s_{21}s_b}{s_{12}} = K_u s_b \quad (7)$$

The selected-fit on-rate (7) just depends on the equilibrium constant  $K_u$  of the conformations  $E_1$  and  $E_2$  in the unbound state, and the binding rate  $s_b$  of the conformation  $E_2$ . Since the equilibrium probability  $P(E_2) = [E_2]/([E_1] + [E_2])$  of conformation  $E_2$  is approximately  $P(E_2) \approx [E_2]/[E_1] = K_u$  for  $[E_2] \ll [E_1]$ , the selected-fit on-rate (7) can also be directly understood as the product of the probability that the

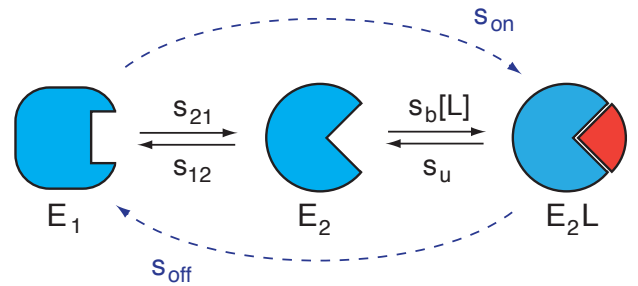
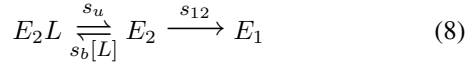


FIG. 2: Binding kinetics along the selected-fit route of our model (see fig. 1). Here,  $s_{21}$  and  $s_{12}$  are the rates for the conformational transitions in the unbound state,  $s_b$  is the binding rate of conformation  $E_2$  per mole ligand, and  $s_u$  the unbinding rate. Since  $E_1$  is the ground state and  $E_2$  the excited state, we have  $K_u = s_{21}/s_{12} \ll 1$ . If the conformational transition rate  $s_{12}$  into the ground state is much larger than the binding and unbinding rates  $s_b[L]$  and  $s_u$ , the on-rate along the selected-fit route is approximately  $s_{\text{on}} \approx K_u s_b$ , and the off-rate is  $s_{\text{off}} \approx s_u$  (see eqs. (7) and (9)).

protein is in conformation  $E_2$  and the binding rate  $s_b$  of this conformation.

The selected-fit off-rate is the dominant relaxation rate of the process



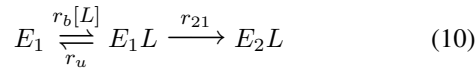
from  $E_2L$  to the  $E_1$ . This process follows the same general reaction scheme as the binding process (5). A reasonable, simplifying assumption here is that the conformational relaxation process from the excited state  $E_2$  to the ground state  $E_1$  is significantly faster than the binding and unbinding process, which implies  $s_{12} \gg s_u$  and  $s_{12} \gg s_b[L]$ . The selected-fit off-rate then simply is

$$\boxed{s_{\text{off}} \approx s_u} \quad (9)$$

(see eq. (26) in the Appendix). The off-rate  $s_{\text{off}}$  thus is independent of the conformational transition rates between  $E_1$  and  $E_2$ . The off-rate is identical with the rate  $s_u$  for the bottleneck step, the unbinding process from  $E_2L$  to  $E_2$ .

### Induced-fit binding kinetics

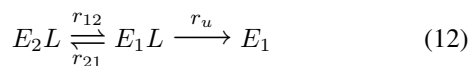
The on-rate along the induced-fit binding route of our model (see figs. 1 and 3) is the dominant relaxation rate of the process



Here,  $r_b$  is the binding rate of conformation  $E_1$  per mole ligand,  $r_u$  is the unbinding rate, and  $r_{21}$  is the rate for the conformational transition into the bound ground state  $E_2L$ . The induced-fit binding process (10) is similar to the selected-fit unbinding process (8). As before, we assume that the conformational transition into the ground state is much faster than the binding and unbinding processes, i.e. we assume  $r_{21} \gg r_b[L]$  and  $r_{21} \gg r_u$ . The induced-fit on-rate per mole ligand then is (see Appendix)

$$\boxed{r_{\text{on}} \approx r_b} \quad (11)$$

The induced-fit unbinding rate is the dominant relaxation rate of the process



which is similar to the selected-fit binding process (5). Since  $E_2L$  is the ground-state conformation in the bound state of the protein, we have  $K_b = r_{21}/r_{12} \gg 1$ . The dominant relaxation rate of (12) then is

$$r_{\text{off}} \approx \frac{r_{12}r_u}{r_{21} + r_u} \quad (13)$$

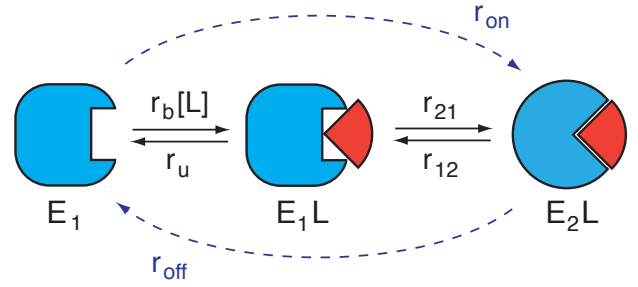


FIG. 3: Binding kinetics along the induced-fit route of our model (see fig. 1). Here,  $r_{12}$  and  $r_{21}$  are the rates for the conformational transitions in the bound state,  $r_b$  is the binding rate of conformation  $E_1$  per mole ligand, and  $r_u$  is the unbinding rate. Because  $E_2L$  is the ground state, we have  $K_b = r_{21}/r_{12} \gg 1$ . For conformational transition rates  $r_{21}$  into the bound ground state that are much larger than the binding and unbinding rates  $r_b[L]$  and  $r_u$ , the on- and off-rates along the induced-fit route are approximately  $r_{\text{on}} \approx r_b$  and  $r_{\text{off}} \approx s_u/K_b$  (see eqs. (11) and (14)).

(see eq. (25) in the Appendix). For fast conformational relaxation into the bound ground state with rate  $r_{21} \gg r_u$ , the induced-fit off-rate is approximately

$$\boxed{r_{\text{off}} \approx \frac{r_u}{K_b}} \quad (14)$$

The off-rate  $r_u/K_b$  can again be understood as the product of the unbinding rate  $r_u$  in the excited state  $E_1L$  and the equilibrium probability  $P(E_1L) = [E_1L]/([E_1L] + [E_2L])$  of this state, which is approximately  $P(E_1L) \approx [E_1L]/[E_2L] = 1/K_b$ .

### Mutational analysis of the binding kinetics

A mutational analysis of the binding kinetics may reveal the characteristic differences between the selected-fit and induced-fit on-rates (7) and (11) and off-rates (9) and (14). Of particular interest here are mutations of residues far away from the ligand-binding site that affect the rate constants for transitions between the conformations, but not the binding rates  $s_b$  and  $r_b$  and unbinding rates  $s_u$  and  $r_u$  of the two conformations. The mutations will change the free-energy differences  $\Delta G_u = G(E_2) - G(E_1)$  and  $\Delta G_b = G(E_2L) - G(E_1L)$  between the two conformations in the unbound and the bound state. In terms of these free-energy differences, the equilibrium constants  $K_u$  and  $K_b$  for the conformational transitions are

$$K_u = RT \exp(-\Delta G_u/RT) \quad \text{and} \quad K_b = RT \exp(-\Delta G_b/RT) \quad (15)$$

From eq. (7), we find that the ratio of the selected-fit on-rates for wildtype and mutant

$$\boxed{\frac{s'_{\text{on}}}{s_{\text{on}}} = \frac{K'_u}{K_u} = \exp(-\Delta\Delta G_u/RT)} \quad (16)$$

depends on the mutation-induced shift  $\Delta\Delta G_u = \Delta G'_u - \Delta G_u$  of the free energy difference between the conformations in the unbound state. The prime here indicates the conformational free-energy difference for the mutant. From eq. (14), we obtain the relation

$$\frac{r'_{\text{off}}}{r_{\text{off}}} = \frac{K_b}{K'_b} = \exp(\Delta\Delta G_b/RT) \quad (17)$$

between the induced-fit off-rates of wildtype and mutant. Here,  $\Delta\Delta G_b = \Delta G'_b - \Delta G_b$  is the mutation-induced shift of the conformational free-energy difference in the bound state. The selected-fit off-rate (9) and induced-fit on-rate (11), in contrast, are the same for wildtype and mutant if the mutations do not affect the binding and unbinding rates of the two conformations.

## DISCUSSION AND CONCLUSIONS

Empirical methods to calculate mutation-induced stability changes of proteins have been investigated intensively in the past years [20, 21, 22, 23, 24, 25, 26, 27, 28, 29]. These methods can be used to calculate the changes  $\Delta\Delta G_u$  of the conformational free-energy difference in the unbound state, provided that experimental protein structures are available both for the unbound and ligand-bound state of the protein. The experimental structure of the protein in the ligand-bound state then corresponds to the excited-state conformation in the unbound state of our model. Calculations of mutation-induced changes  $\Delta\Delta G_b$  of conformational free-energy differences in the bound state are more difficult and require a construction of a ligand-bound excited-state conformation by docking the ligand to the experimental structure of the unbound protein.

In combination with eqs. (16) and (17) of our model, calculated free-energy changes may help to identify selected-fit or induced-fit mechanisms of protein binding. A promising candidate is the protein DHFR, which has been studied extensively as a model enzyme to understand the relations between conformational dynamics, binding, and function. The enzymatic mechanism and conformational changes of DHFR have been investigated by mutational analyses [30, 31, 32, 33, 34], NMR relaxation [16, 17, 35], single-molecule fluorescence experiments [10], and simulation [36, 37, 38]. The strong effect of point mutations far from the ligand binding site on catalytic rates and binding rates suggests large conformational changes during the catalytic cycle [30, 32, 33, 34, 39], in agreement with experimental structures of DHFR in the unbound and several ligand-bound states [40]. Mutations far from the binding sites of DHFR affect the binding kinetics of the two ligands [31, 32, 33], and NMR relaxation experiments point towards a selected-fit mechanism of ligand binding [16]. However, the mutations seem to affect both the binding and the unbinding rates [31, 32, 33]. This precludes a direct comparison with our model, either because the conformational dynamics is more complex, or because the mutations have an indirect effect on the binding free energies.

We have considered here a simple four-state model of protein-ligand binding. The kinetic and mutational analysis

of this model is partly inspired by previous models of the protein folding kinetics [41, 42]. We have found characteristic kinetic differences between the selected-fit and induced-fit binding routes of this model, which should be observable also in more detailed models of conformational changes and binding. While the timescale of the relevant conformational transitions are in general inaccessible to standard molecular dynamics simulations with atomistic protein models [43], conformational selection during binding has been recently studied by combining atomistic simulations and docking [44, 45, 46]. Large conformational transitions are also intensively studied by normal mode analysis [47, 48], in particular with coarse-grained elastic network models of proteins [49, 50, 51, 52, 53, 54].

## APPENDIX: RELAXATION RATES

### General solution

The binding and unbinding processes of our model have a general reaction scheme of the form



For the selected-fit or induced-fit binding process, state  $A$  corresponds to  $E_1$ , and state  $C$  to  $E_2L$ . For the unbinding processes,  $A$  corresponds to  $E_2L$ , and  $C$  to  $E_1$ . We are interested in the dominant, slowest relaxation rate into state  $C$ . Therefore, the state  $C$  is an ‘‘absorbing’’ state, i.e. the rate from  $C$  back to  $B$  is 0. The probability evolution  $P_A(t)$ ,  $P_B(t)$ , and  $P_C(t)$  of the three states is then governed by the set of master equations

$$\frac{dP_A(t)}{dt} = k_{AB}P_B(t) - k_{BA}P_A(t) \quad (19)$$

$$\frac{dP_B(t)}{dt} = k_{BA}P_A(t) - (k_{AB} + k_{CB})P_B(t) \quad (20)$$

$$\frac{dP_C(t)}{dt} = k_{CB}P_B(t) \quad (21)$$

where  $k_{ij}$  denotes the rate from state  $j$  to state  $i$ . The three equations can be written in the matrix form

$$\frac{d\mathbf{P}(t)}{dt} = -\mathbf{W}\mathbf{P}(t) \quad (22)$$

with  $\mathbf{P}(t) = (P_A(t), P_B(t), P_C(t))$  and

$$\mathbf{W} = \begin{pmatrix} k_{BA} & -k_{AB} & 0 \\ -k_{BA} & k_{AB} + k_{CB} & 0 \\ 0 & -k_{CB} & 0 \end{pmatrix} \quad (23)$$

The general solution of (22) has the form [55]

$$\mathbf{P}(t) = c_o\mathbf{Y}_o + c_1\mathbf{Y}_1e^{-\lambda_1 t} + c_2\mathbf{Y}_2e^{-\lambda_2 t} \quad (24)$$

where  $\mathbf{Y}_o$ ,  $\mathbf{Y}_1$ , and  $\mathbf{Y}_2$  are the three eigenvectors of the matrix  $\mathbf{W}$ , and  $\lambda_1$  and  $\lambda_2$  are the two positive eigenvalues of the eigenvectors  $\mathbf{Y}_1$  and  $\mathbf{Y}_2$ . The coefficients  $c_o$ ,  $c_1$ , and  $c_2$

depend on the initial conditions at time  $t = 0$ . The eigenvalue of the eigenvector  $\mathbf{Y}_o$  is 0, which ensures that  $\mathbf{P}(t)$  relaxes towards a finite equilibrium probability distribution  $\mathbf{P}(t \rightarrow \infty) = c_o \mathbf{Y}_o$  for  $t \rightarrow \infty$ . The two nonzero eigenvalues are

$$\lambda_{1/2} = \frac{1}{2} \left( k_{AB} + k_{BA} + k_{CB} \pm \sqrt{k_{AB}^2 + (k_{BA} - k_{CB})^2 + 2k_{AB}(k_{BA} + k_{CB})} \right)$$

These eigenvalues, and their eigenvectors  $\mathbf{Y}_1$  and  $\mathbf{Y}_2$ , capture the time-dependent relaxation process into equilibrium (see eq. (24)).

### Selected-fit binding and induced-fit unbinding

In selected-fit binding (5), state  $A$  corresponds to  $E_1$ , state  $B$  to  $E_2$ , and  $C$  to  $E_2L$  (see fig. 1). In induced-fit unbinding (12),  $A$  corresponds to  $E_2L$ ,  $B$  to  $E_1L$  and  $C$  to  $E_1$ . In our model, we have  $[E_2] \ll [E_1]$  and  $[E_2L] \gg [E_1L]$  in equilibrium, which implies  $k_{BA} \ll k_{AB}$  in both cases. The nonzero eigenvalues then are approximately

$$\lambda_1 \approx \frac{k_{BA}k_{CB}}{k_{AB} + k_{CB}} \quad \text{and} \quad \lambda_2 \approx k_{AB} + k_{CB} \quad (25)$$

For  $k_{BA} \ll k_{AB}$ , we have  $\lambda_1 \ll \lambda_2$ . The smaller rate  $\lambda_1$  is the dominant relaxation rate for the initial conditions

$\mathbf{P}(0) = (1, 0, 0)$  (only state  $A$  populated) or  $\mathbf{P}(0) = (1 - k_{BA}/k_{AB}, k_{BA}/k_{AB}, 0)$  ('pre-equilibration' of states  $A$  and  $B$ ). For both initial conditions, the probability evolution of state  $C$  is approximately given by  $P_C(t) \approx 1 - \exp[-\lambda_1 t]$ . The dominant relaxation rate  $\lambda_1$  of eq. (25) can also be obtained from eqs. (19) to (21) in a steady-state approximation, i.e. under the assumption that the variation  $dP_B(t)/dt$  of the intermediate state  $B$  is negligibly small.

### Selected-fit unbinding and induced-fit binding

In selected-fit unbinding (8), the rate  $k_{CB}$  corresponds to  $s_{12}$ , the rate from the excited state  $E_2$  in the unbound ground state  $E_1$ . In induced-fit binding (10),  $k_{CB}$  corresponds to  $r_{21}$ , the rate from  $E_1L$  in the bound ground state  $E_2L$ . We assume here that the rates for these conformational transitions into the ground state are much larger than the binding and unbinding rates. This implies  $k_{AB} \ll k_{CB}$  and  $k_{BA} \ll k_{CB}$ . The nonzero eigenvalues then simply are

$$\lambda_1 \approx k_{BA} \quad \text{and} \quad \lambda_2 \approx k_{CB} \quad (26)$$

with the clearly smaller eigenvalue  $\lambda_1$  as the dominant rate of the relaxation process from state  $A$  to  $C$ .

- 
- [1] Gerstein, M. and Krebs, W. A database of macromolecular motions. *Nucleic Acids Res.* 26:4280–4290, 1998.
- [2] Goh, C.-S., Milburn, D., and Gerstein, M. Conformational changes associated with protein-protein interactions. *Curr. Opin. Struct. Biol.* 14:104–109, 2004.
- [3] Koshland, D. E. Application of a theory of enzyme specificity to protein synthesis. *Proc. Natl. Acad. Sci. USA* 44:98–104, 1958.
- [4] Tsai, C. J., Kumar, S., Ma, B., and Nussinov, R. Folding funnels, binding funnels, and protein function. *Protein Sci.* 8:1181–1190, 1999.
- [5] Tsai, C. J., Ma, B., Sham, Y. Y., Kumar, S., and Nussinov, R. Structured disorder and conformational selection. *Proteins* 44:418–427, 2001.
- [6] Dill, K. A. and Chan, H. S. From Levinthal to pathways to funnels. *Nat. Struct. Biol.* 4:10–19, 1997.
- [7] Bryngelson, J. D., Onuchic, J. N., Soccia, N. D., and Wolynes, P. G. Funnels, pathways, and the energy landscape of protein folding: a synthesis. *Proteins* 21:167–195, 1995.
- [8] Lu, H. P., Xun, L., and Xie, X. S. Single-molecule enzymatic dynamics. *Science* 282:1877–1882, 1998.
- [9] Ha, T., Ting, A. Y., Liang, J., Caldwell, W. B., Deniz, A. A., Chemla, D. S., Schultz, P. G., and Weiss, S. Single-molecule fluorescence spectroscopy of enzyme conformational dynamics and cleavage mechanism. *Proc. Natl. Acad. Sci. USA* 96:893–898, 1999.
- [10] Antikainen, N. M., Smiley, R. D., Benkovic, S. J., and Hammes, G. G. Conformation coupled enzyme catalysis: single-molecule and transient kinetics investigation of dihydrofolate reductase. *Biochemistry* 44:16835–16843, 2005.
- [11] Min, W., English, B. P., Luo, G., Cherayil, B. J., Kou, S. C., and Xie, X. S. Fluctuating enzymes: lessons from single-molecule studies. *Acc. Chem. Res.* 38:923–931, 2005.
- [12] Michalet, X., Weiss, S., and Jager, M. Single-molecule fluorescence studies of protein folding and conformational dynamics. *Chem. Rev.* 106:1785–1813, 2006.
- [13] Smiley, R. D. and Hammes, G. G. Single molecule studies of enzyme mechanisms. *Chem. Rev.* 106:3080–3094, 2006.
- [14] Eisenmesser, E. Z., Bosco, D. A., Akke, M., and Kern, D. Enzyme dynamics during catalysis. *Science* 295:1520–1523, 2002.
- [15] Wang, C., Karpowich, N., Hunt, J. F., Rance, M., and Palmer, A. G. Dynamics of ATP-binding cassette contribute to allosteric control, nucleotide binding and energy transduction in ABC transporters. *J. Mol. Biol.* 342:525–537, 2004.
- [16] Boehr, D. D., McElheny, D., Dyson, H. J., and Wright, P. E. The dynamic energy landscape of dihydrofolate reductase catalysis. *Science* 313:1638–1642, 2006.
- [17] Boehr, D. D., Dyson, H. J., and Wright, P. E. An NMR perspective on enzyme dynamics. *Chem. Rev.* 106:3055–3079, 2006.
- [18] Henzler-Wildman, K. and Kern, D. Dynamic personalities of proteins. *Nature* 450:964–972, 2007.
- [19] Holmes, K. C., Angert, I., Kull, F. J., Jahn, W., and Schroder, R. R. Electron cryo-microscopy shows how strong binding of

- myosin to actin releases nucleotide. *Nature* 425:423–427, 2003.
- [20] Guerois, R., Nielsen, J. E., and Serrano, L. Predicting changes in the stability of proteins and protein complexes: a study of more than 1000 mutations. *J. Mol. Biol.* 320:369–387, 2002.
- [21] Schymkowitz, J., Borg, J., Stricher, F., Nys, R., Rousseau, F., and Serrano, L. The FoldX web server: an online force field. *Nucleic Acids Res.* 33:W382–W388, 2005.
- [22] Gromiha, M. M., Oobatake, M., Kono, H., Uedaira, H., and Sarai, A. Role of structural and sequence information in the prediction of protein stability changes: comparison between buried and partially buried mutations. *Protein Eng.* 12:549–555, 1999.
- [23] Gilis, D. and Rooman, M. PoPMuSiC, an algorithm for predicting protein mutant stability changes: application to prion proteins. *Protein Eng.* 13:849–856, 2000.
- [24] Zhou, H. and Zhou, Y. Distance-scaled, finite ideal-gas reference state improves structure-derived potentials of mean force for structure selection and stability prediction. *Protein. Sci.* 11:2714–2726, 2002.
- [25] Capriotti, E., Fariselli, P., and Casadio, R. I-Mutant2.0: predicting stability changes upon mutation from the protein sequence or structure. *Nucleic Acids Res.* 33:W306–W310, 2005.
- [26] Cheng, J., Randall, A., and Baldi, P. Prediction of protein stability changes for single-site mutations using support vector machines. *Proteins* 62:1125–1132, 2006.
- [27] Huang, L.-T., Saraboji, K., Ho, S.-Y., Hwang, S.-F., Ponnuswamy, M. N., and Gromiha, M. M. Prediction of protein mutant stability using classification and regression tool. *Biophys. Chem.* 125:462–470, 2007.
- [28] Parthiban, V., Gromiha, M. M., Hoppe, C., and Schomburg, D. Structural analysis and prediction of protein mutant stability using distance and torsion potentials: role of secondary structure and solvent accessibility. *Proteins* 66:41–52, 2007.
- [29] Bueno, M., Camacho, C., and Sancho, J. SIMPLE estimate of the free energy change due to aliphatic mutations: Superior predictions based on first principles. *Proteins* 68:850–862, 2007.
- [30] Cameron, C. E. and Benkovic, S. J. Evidence for a functional role of the dynamics of glycine-121 of *Escherichia coli* dihydrofolate reductase obtained from kinetic analysis of a site-directed mutant. *Biochemistry* 36:15792–15800, 1997.
- [31] Miller, G. P. and Benkovic, S. J. Deletion of a highly motional residue affects formation of the Michaelis complex for *Escherichia coli* dihydrofolate reductase. *Biochemistry* 37:6327–6335, 1998.
- [32] Miller, G. P. and Benkovic, S. J. Strength of an interloop hydrogen bond determines the kinetic pathway in catalysis by *Escherichia coli* dihydrofolate reductase. *Biochemistry* 37:6336–6342, 1998.
- [33] Miller, G. P., Wahnou, D. C., and Benkovic, S. J. Interloop contacts modulate ligand cycling during catalysis by *Escherichia coli* dihydrofolate reductase. *Biochemistry* 40:867–875, 2001.
- [34] Wang, L., Goodey, N. M., Benkovic, S. J., and Kohen, A. Coordinated effects of distal mutations on environmentally coupled tunneling in dihydrofolate reductase. *Proc. Natl. Acad. Sci. USA* 103:15753–15758, 2006.
- [35] McElheny, D., Schnell, J. R., Lansing, J. C., Dyson, H. J., and Wright, P. E. Defining the role of active-site loop fluctuations in dihydrofolate reductase catalysis. *Proc. Natl. Acad. Sci. USA* 102(14):5032–5037, 2005.
- [36] Agarwal, P. K., Billeter, S. R., Rajagopalan, P. T. R., Benkovic, S. J., and Hammes-Schiffer, S. Network of coupled promoting motions in enzyme catalysis. *Proc. Natl. Acad. Sci. USA* 99:2794–2799, 2002.
- [37] Rod, T. H., Radkiewicz, J. L., and Brooks III, C. L. Correlated motion and the effect of distal mutations in dihydrofolate reductase. *Proc. Natl. Acad. Sci. USA* 100:6980–6985, 2003.
- [38] Chen, J., Dima, R. I., and Thirumalai, D. Allosteric communication in dihydrofolate reductase: signaling network and pathways for closed to occluded transition and back. *J. Mol. Biol.* 374:250–266, 2007.
- [39] Benkovic, S. J., Hammes, G. G., and Hammes-Schiffer, S. Free-energy landscape of enzyme catalysis. *Biochemistry* 47:3317–3321, 2008.
- [40] Sawaya, M. R. and Kraut, J. Loop and subdomain movements in the mechanism of *Escherichia coli* dihydrofolate reductase: crystallographic evidence. *Biochemistry* 36:586–603, 1997.
- [41] Merlo, C., Dill, K. A., and Weikl, T. R.  $\Phi$ -values in protein folding kinetics have energetic and structural components. *Proc. Natl. Acad. Sci. USA* 102:10171–10175, 2005.
- [42] Weikl, T. R. Transition states in protein folding kinetics: Modeling  $\Phi$ -values of small  $\beta$ -sheet proteins. *Biophys. J.* 94:929–937, 2008.
- [43] Karplus, M. and McCammon, J. A. Molecular dynamics simulations of biomolecules. *Nat. Struct. Biol.* 9:646–652, 2002.
- [44] Wong, S. and Jacobson, M. P. Conformational selection in silico: loop latching motions and ligand binding in enzymes. *Proteins* 71:153–164, 2008.
- [45] Wong, C. F., Kua, J., Zhang, Y., Straatsma, T. P., and McCammon, J. A. Molecular docking of balanol to dynamics snapshots of protein kinase A. *Proteins* 61:850–858, 2005.
- [46] Frembgen-Kesner, T. and Elcock, A. H. Computational sampling of a cryptic drug binding site in a protein receptor: explicit solvent molecular dynamics and inhibitor docking to p38 MAP kinase. *J. Mol. Biol.* 359:202–214, 2006.
- [47] Ma, J. Usefulness and limitations of normal mode analysis in modeling dynamics of biomolecular complexes. *Structure* 13:373–380, 2005.
- [48] Case, D. Normal mode analysis of protein dynamics. *Curr. Opin. Struct. Biol.* 4:285–290, 1994.
- [49] Bahar, I. and Rader, A. J. Coarse-grained normal mode analysis in structural biology. *Curr. Opin. Struct. Biol.* 15:586–592, 2005.
- [50] Yang, L., Song, G., and Jernigan, R. L. How well can we understand large-scale protein motions using normal modes of elastic network models? *Biophys. J.* 93:920–929, 2007.
- [51] Tirion, M. Large amplitude elastic motions in proteins from a single-parameter, atomic analysis. *Phys. Rev. Lett.* 77:1905–1908, 1996.
- [52] Bahar, I., Atilgan, A. R., and Erman, B. Direct evaluation of thermal fluctuations in proteins using a single-parameter harmonic potential. *Fold. Des.* 2(3):173–181, 1997.
- [53] Micheletti, C., Carloni, P., and Maritan, A. Accurate and efficient description of protein vibrational dynamics: comparing molecular dynamics and Gaussian models. *Proteins* 55:635–645, 2004.
- [54] Zheng, W., Brooks, B. R., and Hummer, G. Protein conformational transitions explored by mixed elastic network models. *Proteins* 69:43–57, 2007.
- [55] van Kampen, N. G. *Stochastic processes in physics and chemistry*. 3rd ed., Elsevier, Amsterdam, 2007.